Is There an Intrinsic Limit to the Charge-Carrier-Induced Increase of the Curie Temperature of EuO?

T. Mairoser,[1] A. Schmehl,[1,*] A. Melville,[2] T. Heeg,[2] L. Canella,[3] P. Böni,[4] W. Zander,[5] J. Schubert,[5] D. E. Shai,[6] E. J. Monkman,[6] K. M. Shen,[6] D. G. Schlom,[2] and J. Mannhart[1]

[1]*Zentrum für elektronische Korrelation und Magnetismus, Universität Augsburg, Universitätsstraße 1, 86159 Augsburg, Germany*
[2]*Department of Materials Science and Engineering, Cornell University, Ithaca, New York 14853, USA*
[3]*Institut für Radiochemie, Technische Universität München, 85748 Garching, Germany*
[4]*Physik-Department E21, Technische Universität München, 85748 Garching, Germany*
[5]*IBN 1-IT and JARAFIT, Forschungszentrum Jülich GmbH, 52425 Jülich, Germany*
[6]*Department of Physics, Cornell University, Ithaca, New York 14853, USA*

(Received 6 August 2010; published 14 December 2010)

Rare earth doping is the key strategy to increase the Curie temperature (T_C) of the ferromagnetic semiconductor EuO. The interplay between doping and charge carrier density (n), and the limit of the T_C increase, however, are yet to be understood. We report measurements of n and T_C of Gd-doped EuO over a wide range of doping levels. The results show a direct correlation between n and T_C, with both exhibiting a maximum at high doping. On average, less than 35% of the dopants act as donors, raising the question about the limit to increasing T_C.

DOI: 10.1103/PhysRevLett.105.257206 PACS numbers: 75.47.Lx, 75.50.Pp

Increasing the Curie temperature (T_C) of the half-metallic ferromagnetic semiconductor europium monoxide (band gap $E_{gap} = 1.12$ eV at 300 K [1]) is the key problem which has to be addressed to make this versatile material attractive for wide use. EuO offers the third strongest saturation magnetization of all known ferromagnets [2], one of the largest magneto-optic Kerr effects [3], pronounced insulator-to-metal transitions [4] as well as colossal magnetoresistive effects [5]. The recent demonstration of its half-metallic behavior and its structural and electronic compatibility with the technological relevant semiconductors silicon, GaN [6] and GaAs [7] make EuO a promising material for semiconductor-based spintronics. In addition, epitaxially strained EuO has been predicted to be ferroelectric and even multiferroic [8]. Despite these outstanding properties, the potential of EuO critically depends on the improvement of its Curie temperature of 69 K [9]. To address this challenge, several strategies have been proposed and are pursued, including the application of isostatic pressure [10,11], epitaxial strain [12], and charge carrier doping by either oxygen vacancies [13] or by substituting Eu^{2+} with trivalent ions like Fe^{3+} [14], La^{3+}, or Gd^{3+} [15]. As the latter approach potentially offers the easiest way to substantially boost the T_C of EuO, rare earth doping has been extensively studied [6,15–22]. For optimized doping concentrations x in $Eu_{1-x}B_xO$, Curie temperatures have been reported to reach 170 K for $B = Gd$, $x = 0.04$ [21], and 180 K for $B = Fe$, $x = 0.077$ [23]. For doping concentrations exceeding these optimized values, however, the Curie temperature is progressively suppressed, giving rise to a maximum in T_C. Both the increase of T_C and the existence of a maximum of the Curie temperature for optimized doping have been attributed to an indirect exchange interaction, mediated via the conduction electrons. This indirect exchange acts in addition to the direct Heisenberg exchange between the localized $4f$ magnetic moments of the Eu atoms and is supposed to become stronger with increasing carrier density. Several theoretical models have been introduced which describe this indirect exchange interaction and its effects on T_C via an effective charge carrier doping [12,24,25]. In these models, the existence of a maximum of the Curie temperature is associated with a critical carrier density, above which magnetic instabilities [24] or antiferromagnetic ordering [12] reduce the indirect exchange. These models imply the existence of an intrinsic limit on how far the T_C of EuO can be increased by charge carrier doping. Although the change of T_C is ultimately resulting from a change of n, the comparison of experiment and theory has been based on the measurements of the dependence of the T_C on the doping concentration x, assuming that every dopant donates one electron to the EuO conduction band [12,24,25]. To assess the validity of this assumption and to investigate if increasing the carrier density in EuO inevitably leads to a maximum of T_C, we have systematically measured the carrier densities and Curie temperatures of Gd-doped EuO films over a wide range of doping concentrations. These measurements reveal that only a small fraction of the introduced dopants donate electrons to the conduction band. With increasing n, no maximum of T_C is found; T_C shows a maximum only if plotted as a function of the dopant concentration x. These findings open the question of whether the observed maxima of the $T_C(x)$ for various dopants are truly the intrinsic limit for the doping-induced T_C increase of EuO.

Supplementary Materials

Evaluation of the gadolinium content:

Prompt-Gamma Activation Analysis (PGAA) and X-ray Absorption Spectroscopy (XAS) were applied to measure the Gd content *y* in the $Eu_{1-y}Gd_yO$ films. The PGAA measurements were performed at the FRM II neutron source in Garching, Germany, and the XAS measurements at the Canadian Light Source, Saskatoon, Canada. In the PGAA studies, the background signal of the $YAlO_3$ substrates were found to dominate the gamma ray spectra of the $Eu_{1-y}Gd_yO$ films. Only one characteristic Eu peak and one characteristic Gd peak could be identified, which did not allow to analyze the stoichiometry with the desired accuracy.

X-ray absorption spectroscopy was performed on the Eu and Gd $M_{4,5}$ edges between 1100 eV and 1245 eV at the SGM beamline at the Canadian Light Source. The Gd content was determined by comparing the integrated intensities of the Gd $M_{4,5}$ edges versus the Eu $M_{4,5}$ edges, following the method described by Sutarto *et al.* [1] Measurements were performed using total electron yield (TEY) with samples grounded through the contacts, as well as the inverse partial fluorescence yield (IPFY) [2], which was extracted from the oxygen K partial fluorescence yield. To perform our analysis, we subtracted off a linear sloping background (from the Si capping layer) and the extended x-ray absorption fine structure (EXAFS), and used a simple empirical Shirley background to account for the increased absorption after each edge.

An example XAS spectrum taken in total electron yield from a nominally 16% Gd-doped sample is shown in Figure S1, with the red (blue) shaded area representing the integrated intensity of the Eu (Gd), respectively, and the background shown as a dashed line. TEY measurements also revealed small amounts of Eu^{3+} (presumably from Eu_2O_3) which was undetectable by IPFY, suggesting that Eu_2O_3 is associated only with the surface of the film, and likely introduced before or during the capping or by the patterning processes. The Gd content measured using IPFY is consistently smaller than that measured with TEY, and this is accounted for in the reported uncertainties. The origin of this discrepancy could arise from a small amount of

segregation of the Gd to the film surface, or from the partial fluorescence of the partially oxidized Si overlayer on the films. In the unlikely case that the differences are due to doping gradients in the films, the Gd-doping would vary only by a few percent of the total value along the film thickness. This is not expected to alter the sample properties away from a standard behavior and does affect the main results.

A comparison of the Gd-concentration values, measured by XAS in TEY and IPFY, are listed in table 1. Both methods use a Shirley background functions fit to the Eu *M* edges and Eu EXAFS fits atop linear backgrounds to fit the Gd edges. In addition the IPFY values are corrected to account for the non-linearities of the used partial fluorescence yield detector.

The Gd-doping concentrations shown in the figures 2 and 4 are the averaged values from both the TEY and the IPFY measurements. The Gd-contents for doping levels smaller than 2% were calculated using the averaged ratio between the nominal and measured doping concentrations.

Growth regime:

Oxygen vacancies act as electron donors in EuO_{1-x}, and thereby alter the total charge carrier density measured by the Hall effect. As the oxygen stoichiometry of the EuO films cannot directly be measured, one has to minimize the density of the oxygen vacancies to a degree, so that their contribution to the total charge carrier density is negligible and only the Gd doping affects the Curie temperature of the $Eu_{1-y}Gd_yO$ samples. To do so, all films where grown in the adsorption-controlled regime, at which only EuO is adsorbed at the substrate surface and excess Eu metal is re-evaporated [3]. This growth technique provides EuO films with close to perfect oxygen to Eu ratios.

To test if the $Eu_{1-y}Gd_yO$ films of the present study were grown adsorption-controlled at T_{growth}=350º C, a test substrate was heated to the respective temperature and then exposed to an Eu metal flux of $1.1 \bullet 10^{14}$ atoms/s•cm^2 for about 20 minutes in absence of an oxygen partial background pressure. To prevent oxidation and possible loss of deposited Eu, the sample was capped with 20 nm of amorphous Si.

Consequently, the sample was investigated by Rutherford backscattering spectrometry (RBS). The RBS data show that no Eu was deposited onto the substrate. This implies, that all incident Eu has been re-evaporated, demonstrating that a growth temperature of T_{growth}=350º C is sufficient for the adsorption-controlled growth of $Eu_{1-y}Gd_yO$.

This is also corroborated by the XAS measurements, that do not indicate the presence of Eu and Gd oxidation states smaller than 2+. This supports our finding, that the films were grown adsorption controlled and that the films are free of oxygen vacancies in the resolution limit of XAS. Therefore our data is in agreement with the charge carrier density at low temperatures being dominated by electrons originating from Gd dopants.

A third characteristic marker for the adsorption-controlled growth of our films is the film thickness. As in the adsorption controlled growth regime the film thickness is controlled by the background oxygen partial pressure and the growth time, one would expect deviations from the calculated film thicknesses for growth modes other than adsorption control. We do not observe such changes.

Structural quality of the $Eu_{1-y}Gd_yO$ films:

To exclude possible influences of the film microstructure on the measured Curie temperatures and to check for the presence of second phases, all $Eu_{1-y}Gd_yO$ films were investigated using four-circle x-ray diffraction (XRD). All Θ-2Θ scans only show film and substrate peaks, demonstrating the absence of second phases within the resolution limit of XRD. The Θ-2Θ scans of all films investigated in the doping series are shown in figure S2. As a guide to the eye, the possible positions of the polycrystalline bixbyite Gd_2O_3 peaks are marked. As Gd in Gd_2O_3 also is in a 3+ state, the presence of this unwanted second phase would not be detectable in the XAS measurements. Nevertheless, the XRD measurements demonstrate the absence of Gd_2O_3 in the films within the resolution limit of XRD. In addition, rocking curves on the 002 EuO peaks were measured to assess the film quality. All samples exhibit narrow rocking curves (average full width at half maximum (FWHM) ≈ 40 Arcsec.), demonstrating the coherent growth of the $Eu_{1-y}Gd_yO$ films on the (110)

$YAlO_3$ substrates. The films show slight onsets of relaxation, indicated by the widening of the rocking curve peak bases. All films show highly comparable rocking curves with respect to their intensity, shape and FWHM. This demonstrates an almost identical structural quality of all $Eu_{1-y}Gd_yO$ films regardless of the Gd content y. Therefore we assume negligible influences of the $Eu_{1-y}Gd_yO$ film microstructures on the observed T_C changes.

Magnetic characteristics of the $Eu_{1-y}Gd_yO$ films:

The Hall effect was used to measure the charge carrier densities n of the $Eu_{1-y}Gd_yO$ films. At out-of-plane magnetic fields exceeding the saturation field H_{sat} of the samples, the Hall resistance R_H depends linearly on $\mu_0 H$. At these high fields, the film magnetization is saturated, therefore stays constant (M_{sat}), and does not contribute to the change of the effective field in the films. Therefore only those sections of the $R_H(\mu_0 H)$ characteristics can be used for the determination of n that are measured at $|(\mu_0 H)| > H_{sat}$. The out-of-plane saturation fields of all $Eu_{1-y}Gd_yO$ samples were measured using superconducting quantum interference device (SQUID) magnetometry. To extract the film magnetizations, the field dependent magnetization of a $YAlO_3$ substrate was measured and subtracted from the total sample magnetization. An exemplary $M(\mu_0 H)$ characteristic is shown in figure S3. The combined results for $H_{sat}(y)$ of all $Eu_{1-y}Gd_yO$ films are shown in figure S4. All samples show out-of-plane saturation fields in the range of 2.6 T < $|(\mu_0 H_{sat})|$ < 3.2 T.

To determine the Curie temperatures of the $Eu_{1-y}Gd_yO$ films, the temperature dependence of the in-plane magnetization of the samples ($M(T)$) were measured using SQUID magnetometry on samples of about 3.8 mm x 3.8 mm size. The T_Cs were defined by the apparent onsets of spontaneous magnetization. As the Curie temperature of EuO is strongly influenced by external magnetic fields, the $M(T)$ characteristics were acquired in zero applied magnetic field. As the magnetic domain size in EuO films is smaller than 1 µm [4], the $M(B)$ characteristics below T_C do not represent the single-domain magnetization of the $Eu_{1-y}Gd_yO$ films, but are defined by the temperature-dependent domain dynamics. Application of small in-plane background fields (50 - 100 Gauss) lead to $M(B)$ characteristics that show the single domain magnetization of the films. To demonstrate this difference, figure S5 shows a

comparison of the $M(T)$ characteristics of the 10.2 % Gd-doped film measured in zero-field and at an in-plane field of 50 Gauss. The $M(T)$ characteristics of the $Eu_{1-y}Gd_yO$ films measured in small background fields are in good agreement with the reported behavior of Gd-doped EuO films, e.g. as presented in reference 1.

Hall Measurements:

To determine the charge carrier densities of the $Eu_{1-y}Gd_yO$ films, we followed the approach of Shapira *et al.* [5] and used the Hall effect. The measurements were performed on patterned bridges as shown in figure S6. DC currents I_{DC} were applied between the current contacts. The Hall voltages V_{Hall} were measured in dependence of the applied out-of-plane magnetic field on voltage contacts facing each other. From these values the Hall resistances $R_{Hall} = V_{Hall}/I_{DC}$ were calculated. An exemplary $R_{Hall}(\mu_0 H)$ characteristic is depicted in figure S7. From these characteristics the charge carrier densities were extracted using equation 1 of the main manuscript. As described above, only $R_{Hall}(\mu_0 H)$ values were used with $|(\mu_0 H)| > 4\ \mathrm{T} > H_{sat}$. At these fields, the influence from changing sample magnetizations on the derived characteristics can be neglected. All Hall measurements were performed at $T = 4.2$ K. At these low temperatures ($T << T_C$), the anomalous Hall effect is negligible compared to the normal Hall term [5]. Furthermore, at these low temperatures the large energy splitting of the conduction band of about 0.6 eV [6] leads to an intersection of the lower conduction band with the dopant states that above T_C are energetically located closely below conduction band edge (fig. S8). At $T << T_C$ the dopant electrons are therefore completely drained into the conduction band, whereas thermal excitations of electrons from the valence band ($E_g \approx 0.8$ eV at $T = 4.2$ K) are negligible. Therefore the charge carrier density in the conduction band at $T = 4.2$ K is almost exclusively determined by the active dopants [7,8].

As the Hall geometry usually cannot be realized perfectly, one has to take into account contributions to the Hall voltage originating from the current-induced voltage drop along the measurement bridge. To assess these contributions we have measured the magnetic field dependence of the bridge resistance ($R(\mu_0 H)$) of several samples. An exemplary measurement on a $Eu_{1-y}Gd_yO$ film with $y = 0.0965$ is depicted in figure S9. The temperature dependence of the magnetoresistance $MR = (R(0\ \mathrm{T}) - R(8\ \mathrm{T}))/(R(8\ \mathrm{T}))$ shows a maximum of 87.4 % near the curie temperature

but drops to 0.34 % at 4.5 K. At these low temperatures, far below the insulator-to-metal transition, the total bridge resistance in the magnetic field range of 4T ≤ $|\mu_0 H|$ ≤ 8T, which is used to determine the linear slope of the $R_{\mathrm{Hall}}(\mu_0 H)$ characteristics, only changes by 0.2 Ohms. These small changes do not influence the evaluation of the $R_{\mathrm{Hall}}(\mu_0 H)$ characteristics.

References:

1. R. Sutarto *et al.*, *Phys. Rev. B* **80**, 085308 (2009).
2. A. J. Achkar *et al.*, *arXiv:1001.1925* (2010).
3. R. W. Ulbricht *et al.*, *Appl. Phys. Lett.* **93**, 102105 (2008).
4. M. Matsubara *et al.*, *Phys. Rev. B* **81**, 214447 (2010).
5. Y. Shapira *et al.*, *Phys. Rev. B* **8**, 2299 (1973).
6. P. G. Steeneken et al., *Phys. Rev. Lett.* **88**, 047201 (2002).
7. Oliver *et al.*, Phys. Rev. Lett. **24**, 1064 (1970).
8. Oliver *et al.*, Phys. Rev. B **5**, 1078 (1972).

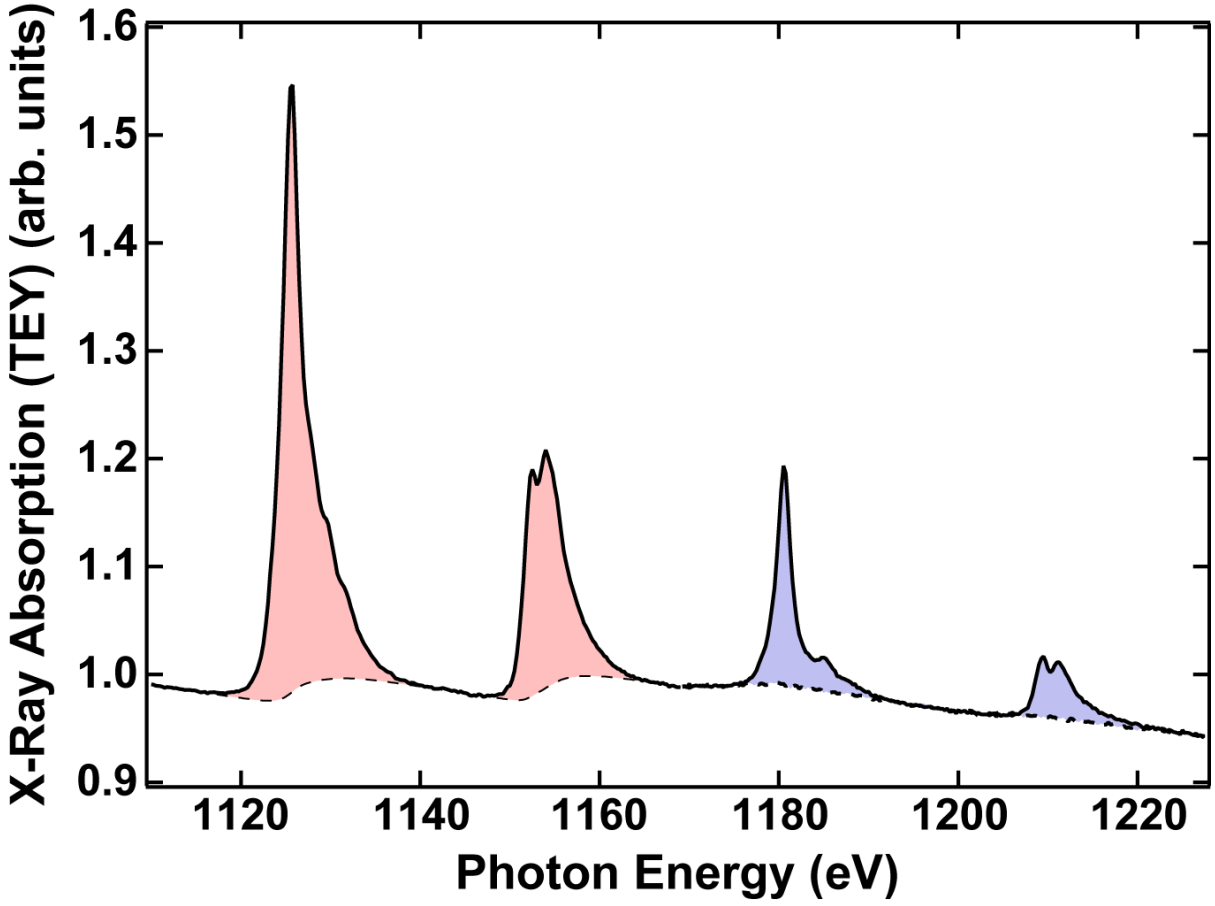
X-Ray Absorption (TEY) (arb. units)
1.6
1.5
1.4
1.3
1.2
1.1
1.0
0.9
1120
1140
1160
1180
1200
1220
Photon Energy (eV)

Figure S1

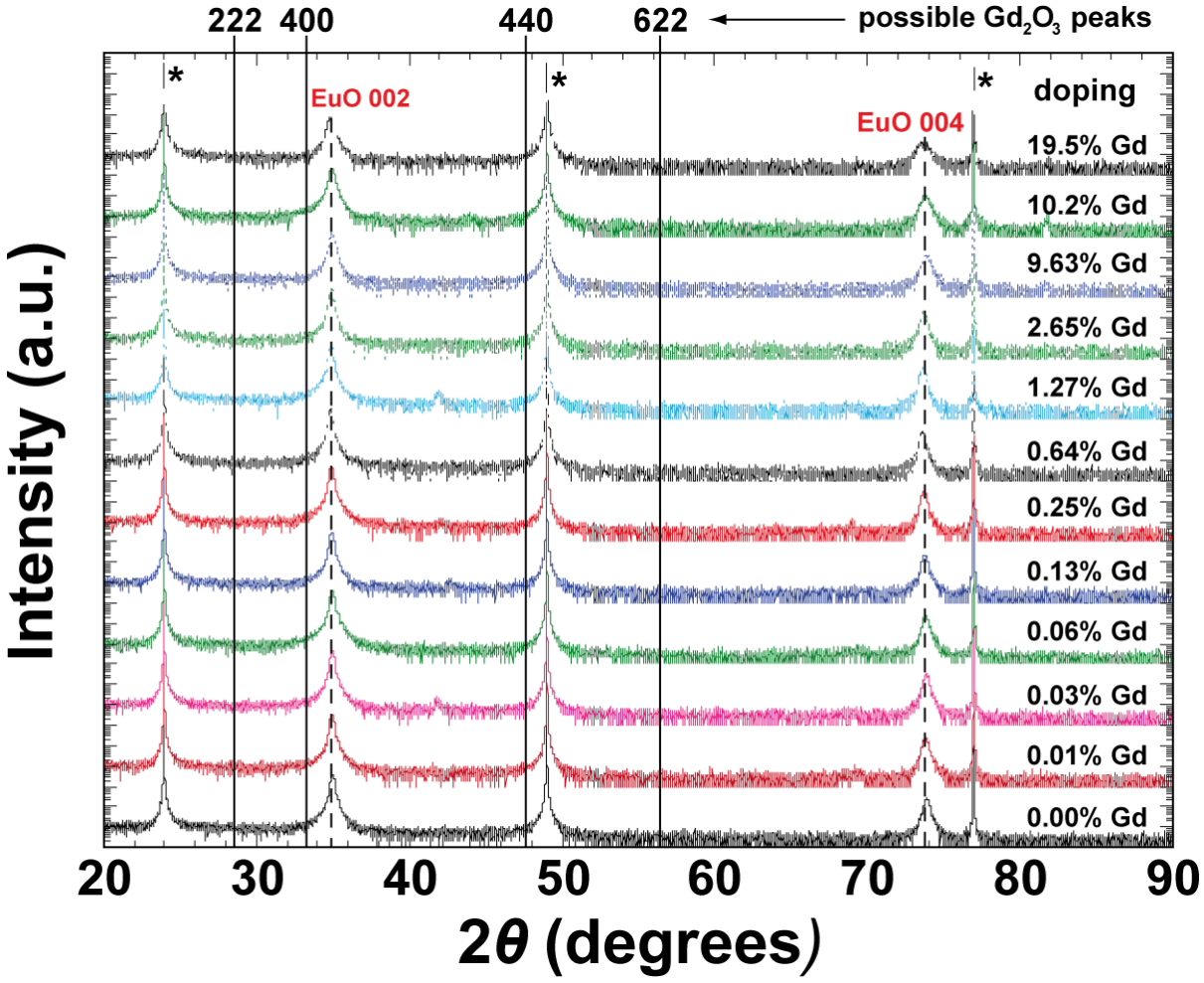
222
400
440
622
possible Gd2O3 peaks
EuO 002
EuO 004
*
doping
19.5% Gd
10.2% Gd
9.63% Gd
2.65% Gd
1.27% Gd
0.64% Gd
0.25% Gd
0.13% Gd
0.06% Gd
0.03% Gd
0.01% Gd
0.00% Gd
Intensity (a.u.)
20
30
40
50
60
70
80
90
2θ (degrees)

Figure S2

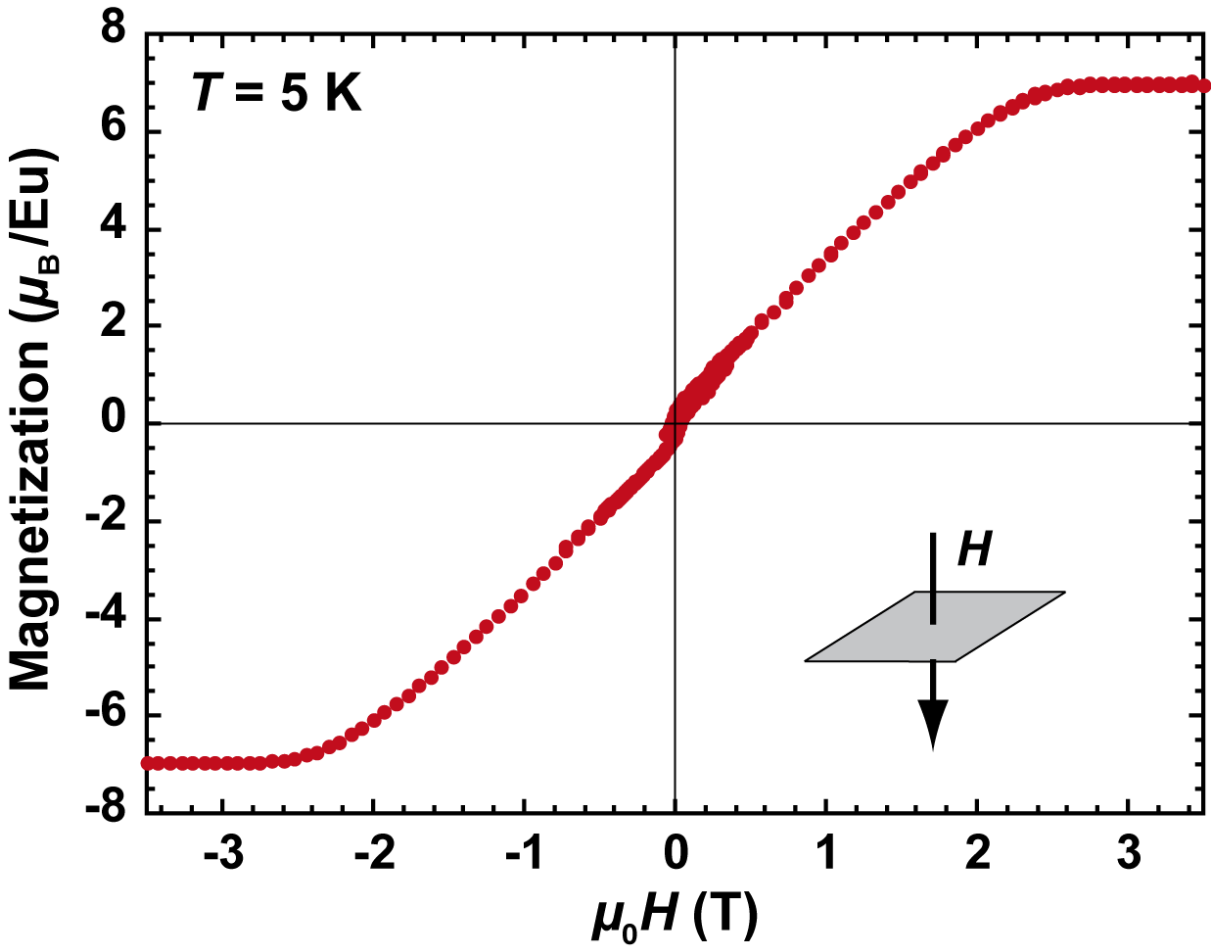

Figure S3

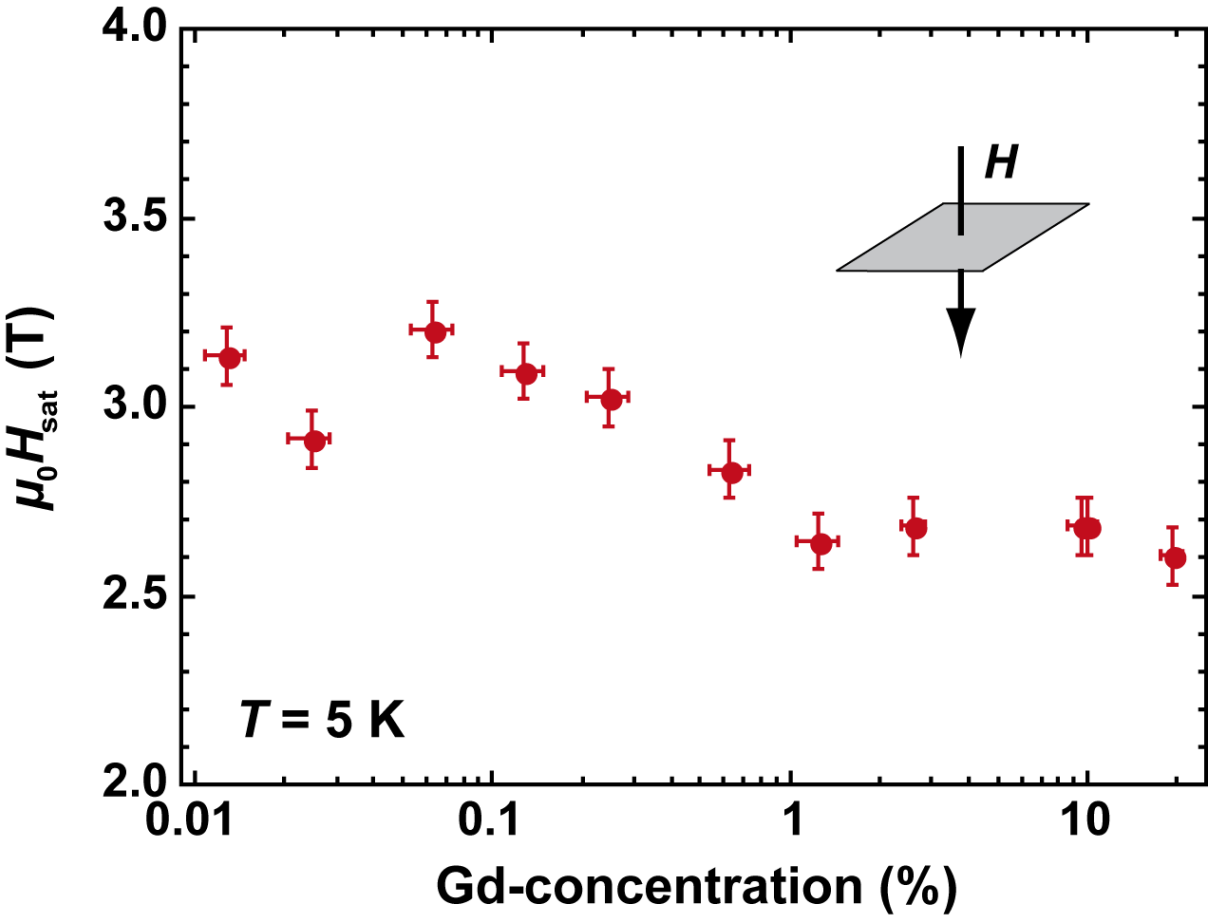

Figure S4

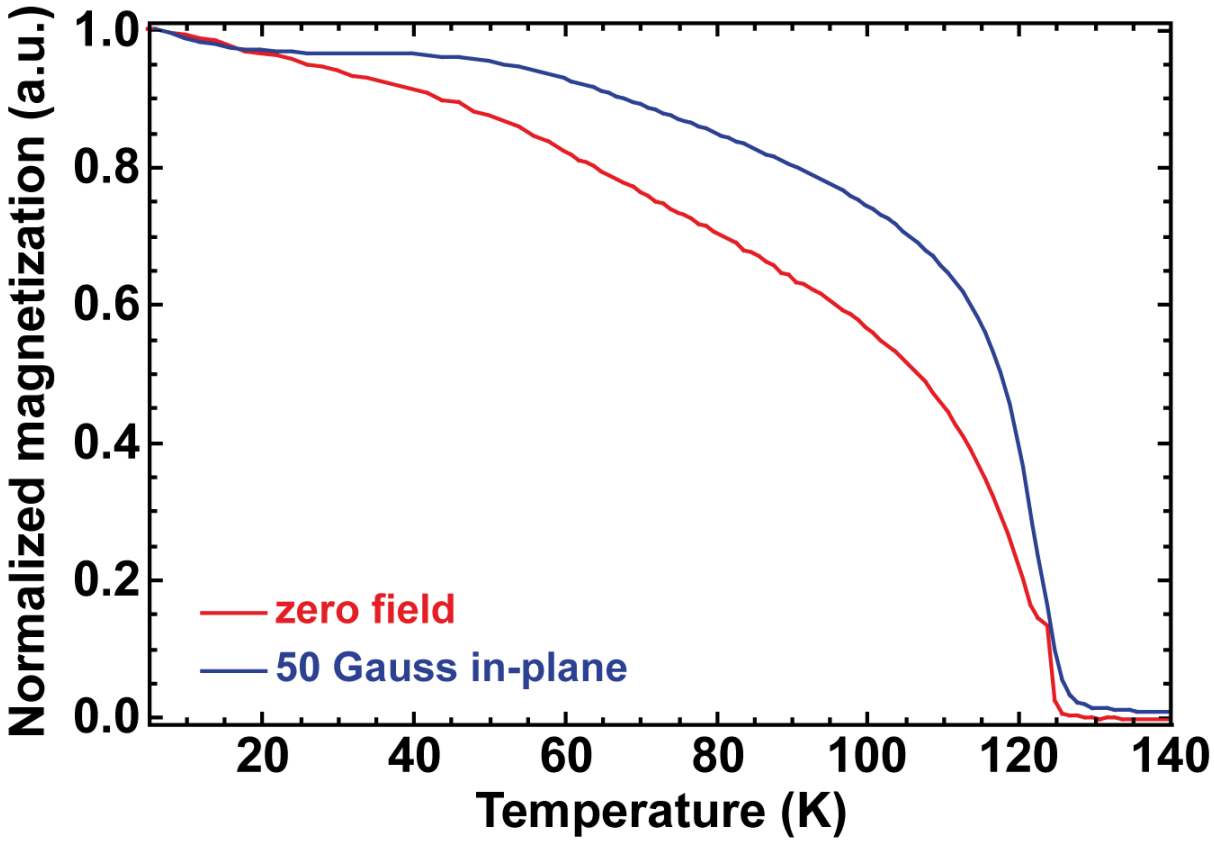
Normalized magnetization (a.u.)
1.0
0.8
0.6
0.4
0.2
0.0
zero field
50 Gauss in-plane
20
40
60
80
100
120
140
Temperature (K)

Figure S5

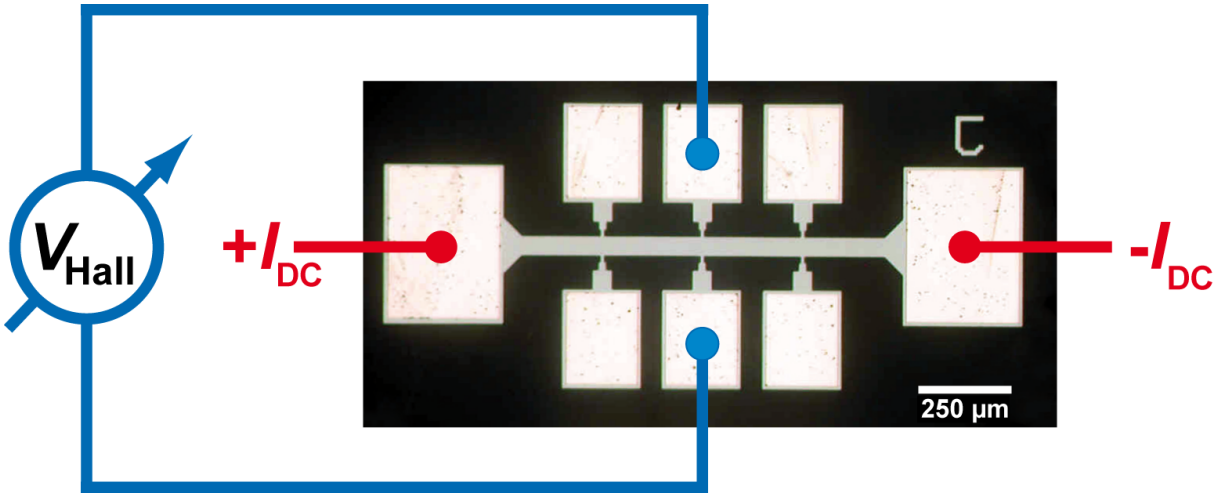

Figure S6

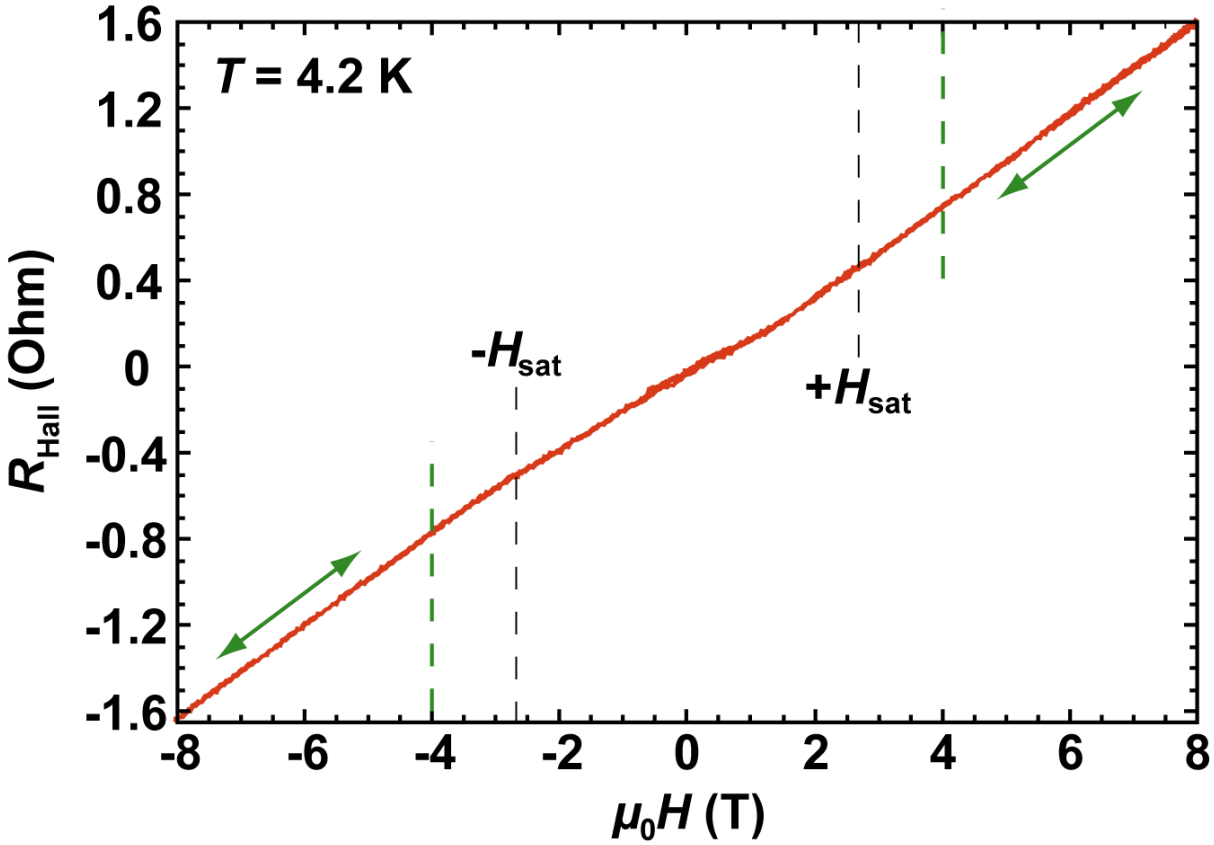
T = 4.2 K
-Hsat
+Hsat
RHall (Ohm)
μ0H (T)
1.6
1.2
0.8
0.4
0
-0.4
-0.8
-1.2
-1.6
-8
-6
-4
-2
0
2
4
6
8

Figure S7

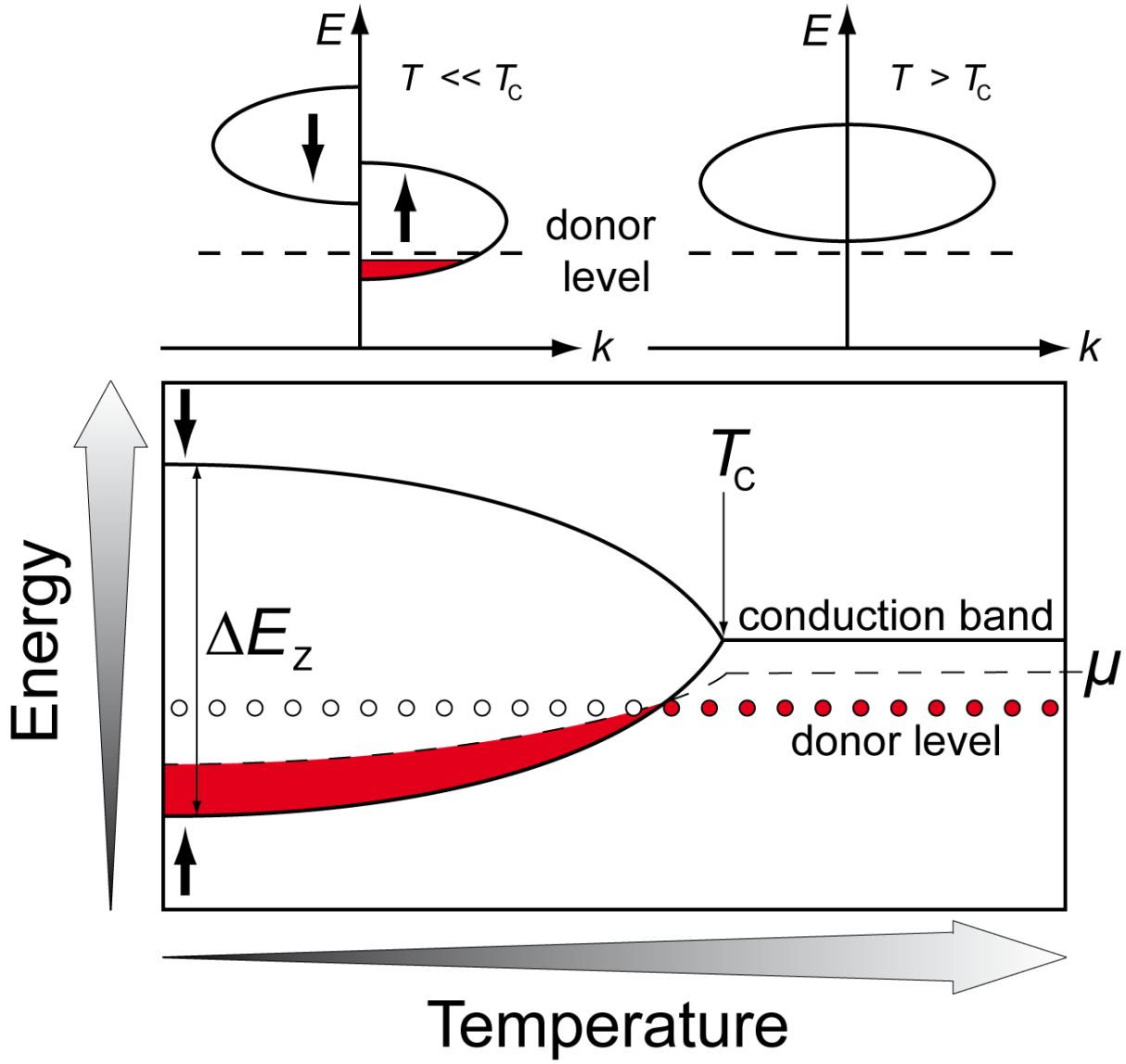
E
T << T_c
E
T > T_c
donor
level
k
k
T_c
ΔE_z
conduction band
μ
donor level
Energy
Temperature

Figure S8

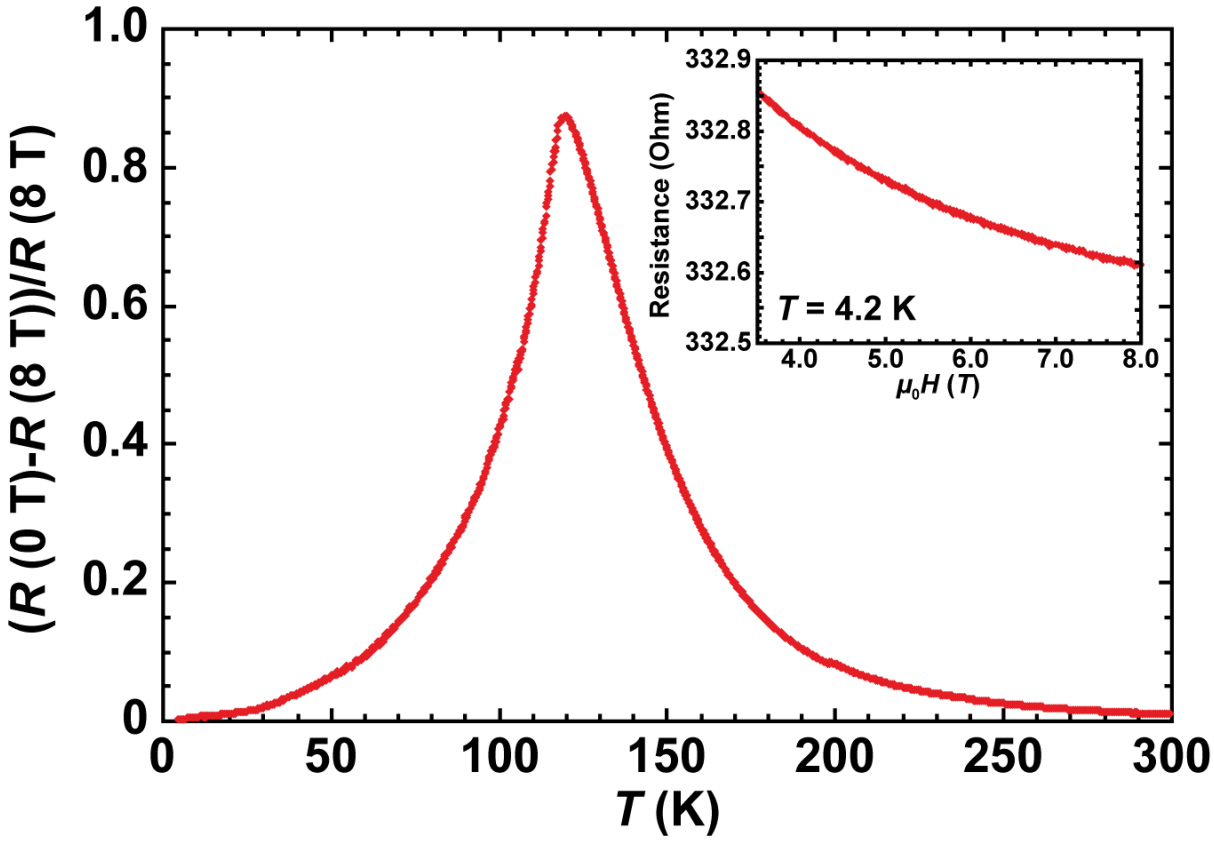

Figure S9

Gd content from XAS in TEY (Shirley background)	Gd content from XAS in IPFY (Shirley background)	Averaged Gd content as presented in the main manuscript
0.0 %	0.0 %	0.00%
2.6 %	2.7 %	2.65 %
10.4 %	8.9 %	9.65 %
10.9 %	9.5 %	10.2 %
21.2 %	17.8 %	19.5 %

Table 1

Captions:

Figure S1: Exemplary XAS spectrum taken in total electron yield (TEY) from a nominally 16% Gd-doped EuO sample. The red (blue) shaded area representing the integrated intensity of the Eu (Gd), respectively, and the background shown as a dashed line.

Figure S2: θ-2θ-scans of all $Eu_{1-y}Gd_yO$ films of the doping series. Only substrate (marked by *) and the 002- and 004-peaks of EuO are present, indicating single phase growth of the film within the resolution limit of XRD. As a guide to the eye, the possible peak positions of polycrystalline bixbyite Gd_2O_3 are marked as well.

Figure S3: Exemplary out-of-plane magnetization curve of a 0.025% Gd-doped EuO film measured at T = 5 K. The substrate contribution to the total magnetization has been subtracted. The film shows a saturation magnetization of 7 μ_B/Eu-Atom with a saturation field of $|\mu_0 H_{sat}|$ = 2.8 T.

Figure S4: Combined results of the out-of-plane saturation fields of all $Eu_{1-y}Gd_yO$ films at T = 5 K. The samples show out-of-plane saturation fields in the range of 2.6 T < $|(\mu_0 H_{sat})|$ < 3.2 T.

Figure S5: Exemplary temperature dependence of the in-plane magnetization of a $Eu_{1-y}Gd_yO$ film (y = 0.102) measured in zero applied magnetic field (red) and with an in-plane background field of 50 Gauss (blue). Even at low background fields the Curie temperature shifts to higher temperatures by several K. The difference in the characteristics below T_C is caused by the suppression of the domain dynamics through the background field.

Figure S6: Schematic of the connection scheme for the Hall measurements (microspcopic picture of an actual bridge structure). DC currents I_{DC} were applied along patterned bridges, and the Hall voltages V_{Hall} measured on facing voltage contacts. From these values the Hall resistances $R_{Hall} = V_{Hall}/I_{DC}$ were calculated.

Figure S7: Exemplary $R_{Hall}(\mu_0 H)$ measurement of a $Eu_{1-y}Gd_yO$ film (y = 0.0965) taken at T = 4.2 K. The shown data consists of two complete measurement loops. To derive charge carrier density, the linear sections of the $R_{Hall}(\mu_0 H)$ characteristic at $|(\mu_0 H)|$ > 4 T where fitted. At these fields substantially above the saturation field H_{sat}, the influence of the sample magnetization can be neglected. As T = 4.2 K << T_C, the contribution of the anomalous Hall effect is negligible, too.

Figure S8: Simplified band structure of electron-doped EuO. Below T_C, the large Zeeman splitting ΔE_Z of the conduction band leads to an intersection of the lower conduction band with the donor level. At T << T_C, the dopant electrons are drained into the conduction band, whereas thermal excitations out of the valence band ($E_g \approx 0.8$ eV at T = 4.2 K) are negligible. Therefore, the charge carrier density in the conduction band is almost exclusively determined by the active dopants.

Figure S9: Exemplary temperature dependence of the magentoresistance of a $Eu_{1-y}Gd_yO$ film with y = 0.0965 (the same sample as shown in figure S7). At low temperatures the magnetic field-induced resistance changes are small, and only amount to 0.2 Ohms at T = 4.2 K in the range of 4 T ≤ $|\mu_0 H|$ ≤ 8 T (inset). These small changes do not influence the evaluation of the $R_{Hall}(\mu_0 H)$ measurements.

Table 1: Comparison of the Gd concentration measured using XAS in total electron yield (TEY) and inverse partial fluorescence yield (IPFY) using Shirley background subtraction. In addition, the IPFY values were corrected to account for the non-linearity of the detector. The Gd contents, as presented in the main letter, were calculated by taking the average of the IPFY and the TEY data.

The $Eu_{1-x}Gd_xO$ films with doping concentrations in the range of $0 \leq x \leq 0.195$ were grown using reactive oxide molecular-beam epitaxy. Gadolinium was chosen as its effects on T_C of EuO have been widely investigated and therefore offers the broadest database of all possible dopants. Europium and gadolinium were coevaporated from effusion cells in oxygen partial background pressures of 1×10^{-9} Torr. The substrate temperature ($T_{\text{growth}} = 350\,^{\circ}\text{C}$) and the oxygen pressure were chosen for adsorption-controlled growth [26] to minimize the density of oxygen vacancies, which would otherwise act as uncontrolled dopants. The incident Eu and Gd fluxes were calibrated using a quartz crystal microbalance and adjusted to result in the desired Gd/Eu ratio (Eu-flux $= 10^{14}$ atoms/cm^2 s). All films were grown to thicknesses d of $\sim$35 nm on (110)-orientated $YAlO_3$ single crystalline substrates [26]. $YAlO_3$ was chosen because of its outstanding insulating properties (band gap = 7.5 eV [27]) which prevent shunting of the highly resistive films at low doping concentrations x. Twelve samples were grown in three batches. The thicknesses of the samples were determined by Rutherford backscattering spectrometry. These thicknesses were assumed to be the same for all films of a batch. The Gd content x for the four samples with the highest doping concentrations was determined by prompt-gamma activation analysis and by the Eu and Gd $M_{4,5}$ edges using x-ray absorption spectroscopy (XAS) [22]. With these values, the average ratio between calibrated Gd flux and measured Gd content was calculated and hence x of the remaining samples determined.

After growth the films were capped *in situ* with $\sim$20 nm of amorphous silicon to prevent oxidation in air. The crystalline quality of all films was examined by four-circle x-ray diffraction. $\theta - 2\theta$ scans demonstrated single-phase films within the resolution limit of XRD. Rocking curves of the 002-peaks indicate that the main fractions of the films are coherently strained by the substrates with a clear onset of relaxation [28]. The in- and out-of-plane magnetic properties of all samples were characterized by superconducting quantum interference device magnetometry [28]. Temperature dependent measurements of the magnetization (zero-field cooled) were used to determine the Curie temperatures of the films. The measured characteristics [Fig. 1(a)] are in agreement with the behavior reported in the literature [6,19,20,22]. Field-dependent magnetization measurements performed at 5 K were used to determine the in-plane and out-of-plane saturation magnetizations (M_{sat}) and fields (H_{sat}). Typical values for $\mu_0 H_{\text{sat}}$ range from 0.12 to 0.19 T for in-plane and 2.6 to 3.2 T for out-of-plane measurements [28].

To measure transport properties, bridges were patterned into the $Eu_{1-x}Gd_xO$ films using photolithography in combination with *in situ* ion-etching and sputter deposition [29]. Low resistance contacts were provided by Mg pads. On the patterned bridges, the temperature dependence of the resistivities [$\rho(T)$] were measured in a four point geometry.

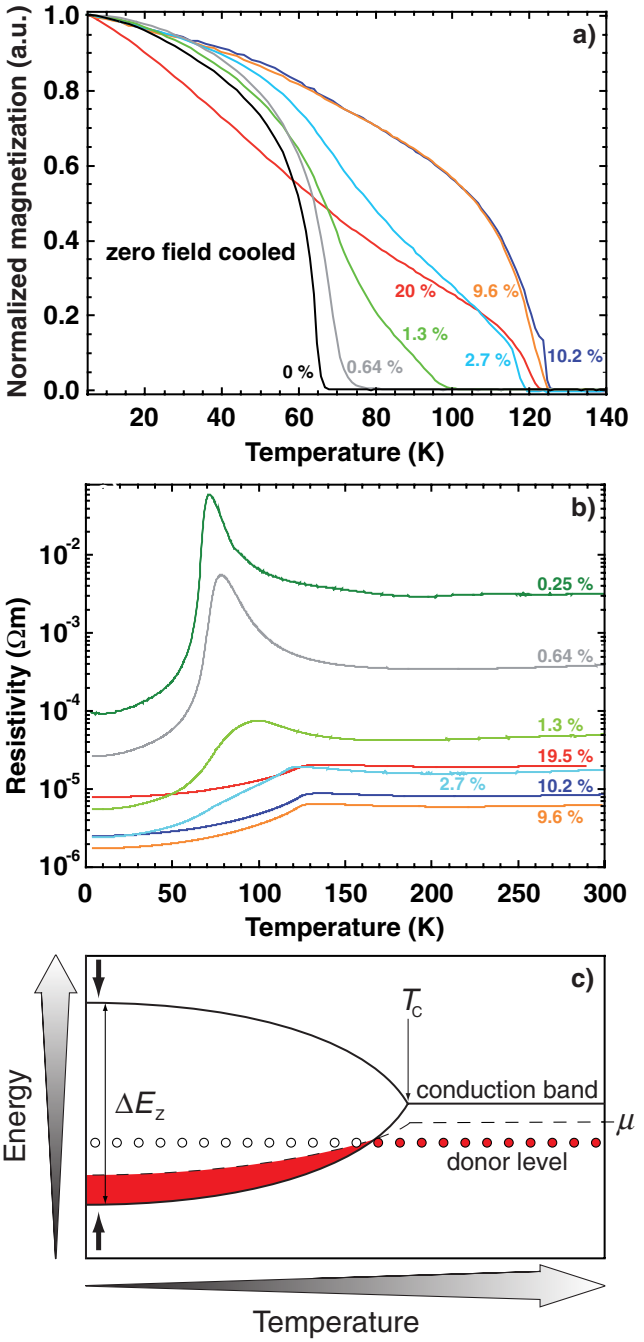

FIG. 1 (color online). (a) temperature dependence of the magnetization of $Eu_{1-x}Gd_xO$ samples measured in zero magnetic field; (b) resistivities of $Eu_{1-x}Gd_xO$ films as a function of temperature; (c) simplified band diagram of Gd-doped EuO. Below T_C the large splitting of the conduction band leads to draining of the dopant electrons into the lower conduction band. For $T \ll T_C$ the carrier density is almost exclusively determined by the active dopants.

Figure 1(b) displays the temperature dependence of the resistivities of $Eu_{1-x}Gd_xO$ films with x in the range of 0.0025 to 0.195. The $\rho(T)$ curves show the typical behavior for doped EuO (see, e.g., [20,30]). For all temperatures, the resistivities strongly depend on the doping concentration x, with a minimum at $x = 0.096$ [Fig. 1(b)].

Out-of-plane magnetic fields H were applied to measure the Hall resistance R_H of the bridges at $T = 4.2$ K [28]. From these measurements the mobile carrier densities n of the films were calculated. At these low temperatures, contributions of the anomalous Hall effect are negligible [5], and for fields above H_{sat}, the Hall resistance depends linearly on the applied magnetic field:

$$R_H(H) = -\frac{1}{end}\mu_0(H + M_{sat}). \quad (1)$$

Here e designates the elementary charge and μ_0 the vacuum permeability. For the determination of n the slopes of $R_H(H)$ were fitted for fields $4\ \mathrm{T} \leq |\mu_0 H| \leq 8\ \mathrm{T}$, well above the measured out-of-plane saturation fields. The measurements were performed on two different bridges on every sample. At $T = 4.2\ \mathrm{K} \ll T_C$, the Zeeman splitting of $\Delta E_Z = 0.6$ eV of the conduction band [31] causes the lower conduction band to intersect with the donor level, which energetically is located closely below the conduction band [Fig. 1(c), [18]]. This induces a charge transfer from the donor levels into the conduction band. At 4.2 K, thermal excitations of electrons from the valence band into the conduction band can be neglected and the measured carrier density originates almost exclusively from electrons donated by the dopants.

The dependence of T_C and n on the doping concentration x are shown in Fig. 2. The data provide evidence that T_C and n are closely correlated. Both increase with x and reach a maximum in the range of $x = 0.10$. The maximum values are $T_C = 129$ K for $x = 0.102$ and $n = 9.0 \times 10^{20}\ \mathrm{cm}^{-3}$ for $x = 0.096$. The $T_C(x)$ dependence is in good agreement with the behavior reported in the literature [17,21,22]. The carrier density measurements, however, reveal that the reduction of T_C at high doping levels is accompanied by a reduction of n. This behavior is in contrast to the existing assumption that the maximum of the $T_C(x)$ characteristics is caused by n exceeding a critical threshold [12,24,25]. The direct correlation of T_C and n is demonstrated in the $T_C(n)$ plot shown in Fig. 3. T_C increases almost logarithmically with n, up to the highest achievable charge carrier densities. A minimum carrier density of $n \sim 1 \times 10^{19}\ \mathrm{cm}^{-3}$ is needed to induce a measurable increase of T_C.

To understand the reduction of n at high doping levels and to assess how many of the dopants donate electrons, we have calculated the expected carrier density n_{ex} assuming that every Gd atom donates one electron into the conduction band according to $n_{ex} = x n_{Eu}$, where n_{Eu} designates the density of Eu atoms in EuO. The ratio of the measured charge density n and the expected charge carrier density therefore provides the fraction of active dopants $p = n/n_{ex}$. The dependence of the dopant activation p on x is shown in Fig. 4. All samples show activations below 35%. After an activation plateau of $p \approx 30\%$ for $0.014 \leq x \leq 0.10$, the sample with the highest doping concentration again shows a strongly reduced activation. For $x = 0.195$, only 10.1% of the dopants donate an electron into the conduction band.

The data indicate that in our samples the reduction of T_C at high doping levels originates from a decrease in dopant activation. This is, in particular, surprising, because the XAS data show no indication of Gd ionization states other than Gd^{3+} [28]. Therefore almost all dopants must have donated one electron. This result implies the existence of charge compensating effects, which block the majority of the donated electrons from being transferred into the conduction band. Only once has a related effect been reported. The origin of this behavior of a Gd-doped EuO crystal has, however, not been identified [16]. As even at the highest doping level neither the $\theta - 2\theta$ scans nor the rocking curves indicate the presence of second phases or a decline in crystalline quality of the $Eu_{1-x}Gd_xO$ films, the origin of the low dopant activation remains an important question.

The results provide a new perspective to utilize rare earth doping to increase T_C in EuO films. In providing a model for the $T_C(x)$ dependence, Mauger, for example,

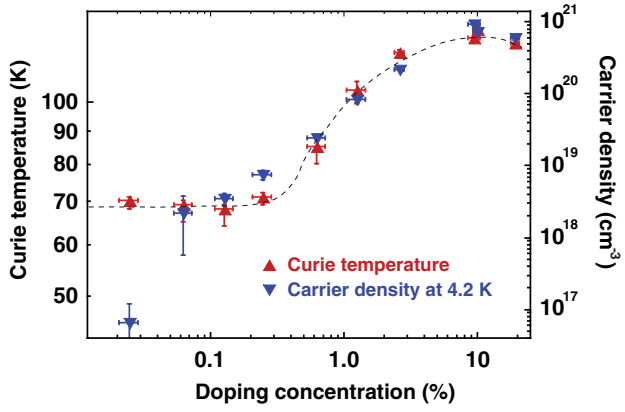

FIG. 2 (color online). Dependence of T_C on x in $Eu_{1-x}Gd_xO$ films measured at 4.2 K. Because of the high sample resistivities at low doping concentrations, charge carrier densities could not be measured for $x < 0.02\%$. The Gd concentrations were determined by XAS. The dotted line is a guide to the eye.

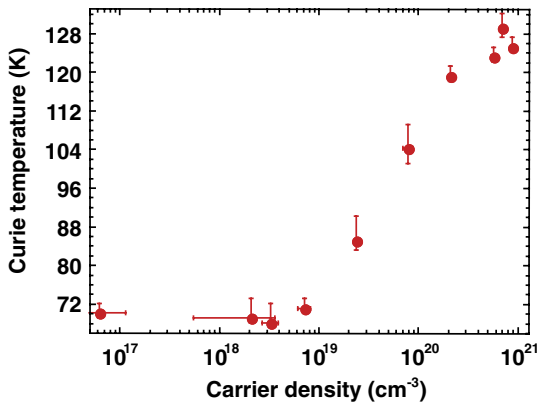

FIG. 3 (color online). Dependence of T_C on n in $Eu_{1-x}Gd_xO$ films. A minimum charge carrier density of $\sim 10^{19}\ \mathrm{cm}^{-3}$ is required to increase T_C above 69 K. For higher concentrations T_C increases approximately logarithmically with n.

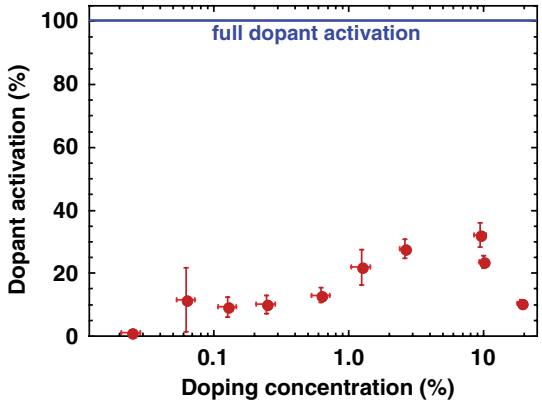

FIG. 4 (color online). Calculated dopant activation p as a function of the doping concentration x in $Eu_{1-x}Gd_xO$.

attributes the existence of the T_C maximum to a spiral instability in the ferromagnetic order along the [111] EuO direction, that is expected to occur for $n > 2 \times 10^{21}$ cm^{-3} [24] ($x > 0.068$ for $p = 1$). In the model developed by Ingle and Elfimov, doping levels $x > 0.08$ ($n > 2.35 \times 10^{21}$ cm^{-3} for $p = 1$) are expected to cause antiferromagnetic order which is postulated to limit T_C to about 150 K [12]. As our samples do not reach such high charge carrier densities but show increasing Curie temperatures with increasing n, they open the question if an intrinsic limit of $T_C(n)$ exists. Furthermore our data indicate that $n > 1 \times 10^{19}$ cm^{-3} is needed to increase T_C (Fig. 3). This finding is in qualitative agreement with the model of Mauger, yet the measured carrier density required is about an order of magnitude smaller than predicted [24].

In conclusion, our measurements of epitaxial $Eu_{1-x}Gd_xO$ films show a close correlation between T_C and n. Our measurements indicate that the maximum in T_C is accompanied by a maximum in n. This would be in contrast to the existing understanding that this maximum is due to the charge carrier density exceeding a critical level. We found that only a small fraction ($< 35\%$) of the introduced dopants acts as donors, whereas the majority of the Gd is rendered inactive. This clearly demonstrates that the widespread assumption of every dopant being a donor is questionable, and that doping experiments to increase the Curie temperature of EuO have to be correlated to the charge carrier density, not only to the doping concentration x. The origin of the low dopant activation has yet to be identified. Furthermore, the data demonstrate that a minimum charge carrier density is required to increase T_C. Finally we want to point out that our data are in very good quantitative agreement with those of [22] and that the Curie temperatures of both experiments are well below the reported maximum T_C for Gd-doped EuO. As latter experiments were performed on polycrystalline films with unknown oxygen stoichiometry, the influence of oxygen vacancies and defects on the dopant activation is an important question to be addressed with respect to the further increase of the Curie temperature of EuO.

We gratefully acknowledge discussions with L. H. Tjeng and thank T. Regier for his assistance in the XAS measurements. This work was supported by the DFG (TRR 80), the EC (oxIDes), AFOSR (FA9550-10-1-0123), and NSF (DMR-0820404).

*andreas.schmehl@physik.uni-augsburg.de

[1] J. O. Dimmock, IBM J. Res. Dev. **14**, 301 (1970).
[2] B. T. Matthias, R. M. Bozorth, and J. H. Van Vleck, Phys. Rev. Lett. **7**, 160 (1961).
[3] K. Y. Ahn and J. C. Suits, IEEE Trans. Magn. **3**, 453 (1967).
[4] M. W. Shafer, J. B. Torrance, and T. Penney, J. Phys. Chem. Solids **33**, 2251 (1972).
[5] Y. Shapira, S. Foner, and T. B. Reed, Phys. Rev. B **8**, 2299 (1973).
[6] A. Schmehl *et al.*, Nature Mater. **6**, 882 (2007).
[7] A. G. Swartz *et al.*, Appl. Phys. Lett. **97**, 112509 (2010).
[8] E. Bousquet, N. A. Spaldin, and P. Ghosez, Phys. Rev. Lett. **104**, 037601 (2010).
[9] T. R. McGuire and M. W. Shafer, J. Appl. Phys. **35**, 984 (1964).
[10] R. Stevenso and M. C. Robinson, Can. J. Phys. **43**, 1744 (1965).
[11] M. M. Abd-Elmeguid and R. D. Taylor, Phys. Rev. B **42**, 1048 (1990).
[12] N. J. C. Ingle and I. S. Elfimov, Phys. Rev. B **77**, 121202 (2008).
[13] K. Y. Ahn and M. W. Shafer, J. Appl. Phys. **41**, 1260 (1970).
[14] K. Y. Ahn, Appl. Phys. Lett. **17**, 347 (1970).
[15] K. Y. Ahn and T. R. McGuire, J. Appl. Phys. **39**, 5061 (1968).
[16] S. von Molnar and M. W. Shafer, J. Appl. Phys. **41**, 1093 (1970).
[17] A. A. Smakhvalov *et al.*, Sov. Phys. Solid State **15**, 2459 (1974).
[18] J. Schoenes and P. Wachter, Phys. Rev. B **9**, 3097 (1974).
[19] A. Mauger *et al.*, J. Phys. (Paris) **39**, 1125 (1978).
[20] T. Matsumoto *et al.*, J. Phys. Condens. Matter **16**, 6017 (2004).
[21] H. Ott *et al.*, Phys. Rev. B **73**, 094407 (2006).
[22] R. Sutarto *et al.*, Phys. Rev. B **80**, 085308 (2009).
[23] K. Y. Ahn, K. N. Tu, and W. J. Reuter, J. Appl. Phys. **42**, 1769 (1971).
[24] A. Mauger, Phys. Status Solidi B **84**, 761 (1977).
[25] M. Arnold and J. Kroha, Phys. Rev. Lett. **100**, 046404 (2008).
[26] R. W. Ulbricht *et al.*, Appl. Phys. Lett. **93**, 102105 (2008).
[27] V. N. Abramov and A. I. Kuznetsov, Fiz. Tverd. Tela (Leningrad) **20**, 689 (1978).
[28] See supplementary material at http://link.aps.org/supplemental/10.1103/PhysRevLett.105.257206 for details.
[29] For more information about patterning process, see supplementary material of Ref. [6].
[30] M. R. Oliver *et al.*, Phys. Rev. B **5**, 1078 (1972).
[31] P. G. Steeneken *et al.*, Phys. Rev. Lett. **88**, 047201 (2002).